Cross-phase modulation and induced focusing due to optical nonlinearities in optical fibers and bulk materials

R. R. Alfano, P. L. Baldeck, and P. P. Ho

Institute for Ultrafast Spectroscopy and Lasers and Photonics Application Laboratory, Department of Electrical Engineering, The City College of New York, New York, New York 10031

Govind P. Agrawal

AT&T Bell Laboratories, Murray Hill, New Jersey 07974

Received October 18, 1988; accepted December 28, 1988

Cross-phase modulation (XPM) and induced focusing occur when copropagating ultrafast pulses interact in a nonlinear medium. XPM and induced focusing are investigated as new techniques to control the spectral, temporal, and spatial properties of ultrafast pulses with femtosecond time response. In this paper we review our most recent measurements on (1) induced spectral broadening in BK7 glass, (2) induced frequency shift of copropagating pulses in optical fibers, (3) XPM-stimulated Raman scattering in optical fibers, (4) XPM second-harmonic generation in ZnSe crystals, and (5) induced focusing of Raman pulses in optical fibers.

1. INTRODUCTION

When an intense ultrashort pulse propagates through a medium, it distorts the atomic configuration of the material, which changes the refractive index. The pulse phase is time and spatially modulated, which affects its spectral, temporal, and spatial properties. Self-phase modulation and self-focusing occur from the phase modulation generated by the pulse itself. Cross-phase modulation (XPM) and induced focusing arise from the phase modulations generated by copropagating pulses. Several schemes of nonlinear interaction between optical pulses can lead to XPM and induced-focusing effects. XPM is intrinsic in the generation processes of stimulated Raman scattering (SRS) pulses, second-harmonic generation (SHG) pulses, and stimulated four-photon mixing pulses. More importantly, the XPM and induced-focusing effects generated by a pump pulse can be used to control, with femtosecond time response, the spectral, temporal, and spatial properties of ultrashort probe pulses.

Early studies of XPM characterized induced polarization effects, such as induced phase changes from the optical Kerr effect, but did not investigate spectral, temporal, and spatial effects on the properties of ultrashort pulses. In 1980, Gersten *et al.*[1] predicted that Raman spectra of ultrashort pulses would be broadened by XPM. The first experimental observation of XPM spectral effects dates to early 1986, when Alfano *et al.*[2] reported that intense picosecond pulses could be used to enhance the spectral broadening of weaker pulses copropagating in bulk glasses.[2,3] Since then, several groups have been studying XPM effects generated by ultrashort pump pulses on copropagating Raman pulses,[4–12] second-harmonic pulses,[13–17] stimulated four-photon mixing pulses,[18] and probe pulses.[2,19] Recently it was shown that XPM leads to the generation of modulation instability,[20–25] solitary waves,[26] and pulse compression.[27–29] Finally, XPM effects on ultrashort pulses have been proposed to tune the frequency of the probe pulse,[30] to eliminate the soliton self-frequency shift effect,[31] and to control the spatial distribution of light in large-core optical fibers.[32–34]

In this paper we review our most recent experimental results, which have contributed to the discovery of spectral, temporal, and spatial effects attributed to XPM and induced focusing. In Section 2 the basis of the XPM theory is outlined. Measurements of spectral-broadening enhancement and induced-frequency shift are presented in Sections 3 and 4, respectively. Sections 5 and 6 consider the effects of XPM on Raman pulses and second-harmonic pulses. Finally, Section 7 shows how the induced focusing of Raman pulses can occur in large-core optical fibers.

2. NONLINEAR POLARIZATION OF COPROPAGATING OPTICAL PULSES

The optical electromagnetic field of two copropagating pulses must ultimately satisfy Maxwell's vector equation

$$\nabla \times \nabla \times E = -\mu_0(\partial D/\partial t), \tag{1a}$$

and

$$D = \epsilon E + P^{\mathrm{NL}}, \tag{1b}$$

where ϵ is the medium permittivity at low intensity and P^{NL} is the nonlinear polarization vector. Assuming a pulse duration that is much longer than the response time of the medium, an isotrope medium, the same linear polarization for the copropagating fields, and no frequency dependence for the nonlinear susceptibility $\chi^{(3)}$, the nonlinear polarization reduces to

$$P^{\mathrm{NL}}(r, z, t) = \chi^{(3)}E^3(r, z, t). \tag{2}$$

0740-3224/89/040824-06$02.00

The transverse component of the total electric field can be approximated by

$$E(r, z, t) = \tfrac{1}{2}\{A_1(r, z, t)\exp[i(\omega_1 t - \beta_1 z)] + A_2(r, z, t)\exp[i(\omega_2 t - \beta_2 z)] + \text{c.c.}\}, \quad (3)$$

where A_1 and A_2 refer to the envelopes of copropagating pulses of carrier frequency ω_1 and ω_2; β_1 and β_2 are the corresponding propagation constants, respectively.

Substituting Eq. (3) into Eq. (2) and keeping only the terms synchronized with ω_1 and ω_2, we obtain

$$P^{\text{NL}}(r, z, t) = P_1^{\text{NL}}(r, z, t) + P_2^{\text{NL}}(r, z, t), \quad (4a)$$

$$P_1^{\text{NL}}(r, z, t) = \tfrac{3}{8}\chi^{(3)}(|A_1|^2 + 2|A_2|^2)A_1 \exp[i(\omega_1 t - \beta_1 z)], \quad (4b)$$

$$P_2^{\text{NL}}(r, z, t) = \tfrac{3}{8}\chi^{(3)}(|A_2|^2 + 2|A_1|^2)A_2 \exp[i(\omega_2 t - \beta_2 z)], \quad (4c)$$

where P_1^{NL} and P_2^{NL} are the nonlinear polarizations at frequencies ω_1 and ω_2, respectively. The second terms on the right-hand sides of Eqs. (4b) and (4c) are XPM terms. Note the factor of 2.

Combining Eqs. (1)–(4) and using the slowly varying envelope approximation (at the first order for the nonlinearity), we obtain the coupled nonlinear wave equations

$$\frac{\partial A_1}{\partial z} + \frac{1}{v_{g1}}\frac{\partial A_1}{\partial t} + i\beta_1^{(2)}\frac{\partial^2 A_1}{\partial t^2} = i\frac{\omega_1}{c}n_2(|A_1|^2 + 2|A_2|^2)A_1, \quad (5a)$$

$$\frac{\partial A_2}{\partial z} + \frac{1}{v_{g2}}\frac{\partial A_2}{\partial t} + i\beta_2^{(2)}\frac{\partial^2 A_2}{\partial t^2} = i\frac{\omega_2}{c}n_2(|A_2|^2 + 2|A_1|^2)A_2, \quad (5b)$$

where v_{gi} is the group velocity for the wave i, $\beta_i^{(2)}$ is the group-velocity dispersion for the wave i, and $n_2 = 3\chi^{(3)}/8n\epsilon_0$ is the nonlinear refractive index.

In the most general case numerical methods are used to solve Eqs. (5). However, they have analytical solutions when the group-velocity dispersion, temporally broadened, can be neglected.[6,8,30]

Figure 1 shows how the spectrum of a weak probe pulse can be affected by the XPM generated by a strong copropagating pulse if group-velocity dispersion temporal broadening can be neglected [$\beta_1^{(2)} = \beta_2^{(2)} = 0$]. The wavelength of the pump pulse was chosen for when the pump pulse travels faster than the probe pulse, $v_{g1} > v_{g2}$. Initial time delays between pulses at the entrance of the nonlinear medium were selected to display the most characteristic interaction schemes. The reference spectrum is shown in Fig. 1(a). Figure 1(b) shows how the probe spectrum changes after the XPM interaction but for a negligible group-velocity mismatch, i.e., no walkoff. The case of no initial time delay and total walkoff is shown in Fig. 1(c). The probe spectrum is shifted and broadened by XPM. The anti-Stokes shift is characteristic of the probe- and pump-pulse walkoff. The probe pulse is blue shifted because it is modulated only by the back of the faster pump pulse as the pump-pulse walkoff. When the time delay is chosen such that the pump pulse enters the nonlinear medium after the probe and just has time to catch up with the probe pulse, we obtain a broadening similar to that of Fig. 1(c) but with a reverse Stokes shift [Fig. 1(d)]. The XPM broadening becomes symmetric when the input time delay allows the pump pulse not only to catch up with but also to pass partially through the probe pulse [Fig. 1(e)]. However, if the interaction length is long enough to allow the pump pulse to overcome the probe pulse completely, there is no XPM-induced broadening [Fig. 1(f)].

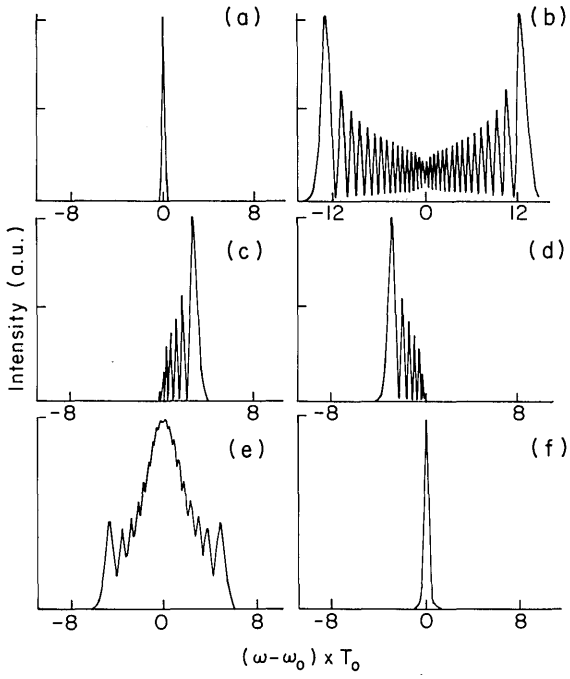

Fig. 1. Influence of XPM, walkoff, and input time delay on the spectrum of a probe pulse from Eqs. (5) with $E_1^2 \gg E_2^2$. $\phi = (\omega_2/c)n_2E_1^2L_w$, $\delta = z/L_w$, and τ_d are the XPM, walkoff, and input time-delay parameters, respectively. (a) Reference spectrum with no XPM, i.e., $\phi = 0$; (b) XPM in the absence of walkoff, i.e., $\phi = 50$ and $\delta = 0$; (c) XPM, total walkoff, and no initial time delay, i.e., $\phi = 50$, $\delta = -5$, and $\tau_d = 0$; (d) XPM and initial time delay to compensate for the walkoff, i.e., $\phi = 50$, $\delta = -5$, and $\tau_d = 5$; (e) XPM and symmetrical partial walkoff, i.e., $\phi = 50$, $\delta = -3$, and $\tau_d = 1.5$; (f) XPM and symmetric total walkoff, i.e., $\phi = 50$, $\delta = -5$, and $\tau_d = 2.5$.

3. SPECTRAL-BROADENING ENHANCEMENT BY CROSS-PHASE MODULATION

XPM causes pulse spectra to broaden more than with self-phase modulation (SPM) only. Using the result of Eqs. (5) and neglecting dispersive effects, we can compute the spectral broadening of a Gaussian pulse at ω_1 by a pump pulse at ω_2 to be

$$\Delta\omega_{1_{\text{SPM+XPM}}} \approx \frac{\omega_1}{c}n_2(|E_1|^2 + 2|E_2|^2)\frac{z}{T_0}. \quad (6)$$

This leads to a spectral-broadening enhancement given by

$$\frac{\Delta\omega_{1_{\text{SPM+XPM}}}}{\Delta\omega_{1_{\text{SPM}}}} = \left(1 + 2\frac{|E_2|^2}{|E_1|^2}\right). \quad (7)$$

The first observation of such a spectral-broadening enhancement was reported in 1986.[2] The spectrum of a 80-μJ picosecond 527-nm pulse weakly focused in a 9-cm-long BK7 glass could be modified by the presence of an intense 2-mJ picosecond pulse at 1054 nm (Fig. 2). This result is important because it could lead to the spectral broadening

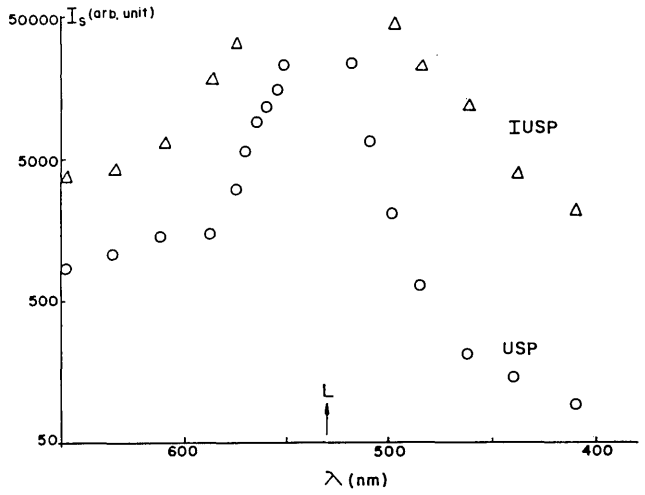

Fig. 2. Intensities of the induced ultrafast supercontinuum pulse (IUSP) and the ultrafast supercontinuum pulse (USP). Each data point was an average of ~20 laser shots and was corrected for the detector, filter, and spectrometer spectral sensitivity. Triangles, IUSP (F_1, 3–75); circles, USP from 527 nm (F_1, HA30). USP from 1054 nm, which is not shown here, was ≈1% of the IUSP signal. The measured 527-nm probe pulse was approximately 5 × 10 counts in this arbitrary unit scale. The error bar of each data point is approximately ±20%.[2]

and pulse compression of weak picosecond pulses generated by diode lasers.

4. INDUCED FREQUENCY SHIFT OF COPROPAGATING PULSES IN OPTICAL FIBERS

XPM effects in dispersive media are affected by the group-velocity mismatch that causes the probe pulse to see only the trailing (or leading) edge of the pump pulse. As a result, the spectral distribution of the probe pulse can be controlled to be blue shifted (or red shifted). However, XPM induces no spectral change when the probe pulse passes entirely through the pump pulse. Recently it was shown that ultrafast pulses overlapping in nonlinear dispersive media undergo a substantial shift of their carrier frequency.[11,30]

A mode-locked Nd:YAG laser with a second-harmonic crystal was used to produce 33-psec infrared pulses and 25-psec green pulses. These pulses were separated using a Mach–Zehnder interferometer delay scheme with wavelength-selective mirrors. The infrared and green pulses propagated in different interferometer arms. The optical path of each pulse was controlled by using variable optical delays. The energy of infrared pulses was adjusted with neutral-density fibers in the range 1–100 nJ, and the energy of green pulses was set to approximately 1 nJ. The nonlinear dispersive medium was a 1-m-long single-mode optical fiber (Corguide, Corning Glass). This length was chosen to allow for total walkoff without loss of control of the pulse delay at the fiber output. The group-velocity mismatch between 532- and 1064-nm pulses was calculated to be approximately 76 psec/m in fused silica. The spectrum of green pulses was measured using a grating spectrometer (1 m, 1200 lines/mm) and an optical multichannel analyzer.

The spectra of green pulses propagating with and without infrared pulses are plotted in Fig. 3. The dashed trace corresponds to the case of green pulses propagating alone. The blue-shifted and red-shifted spectra are those of green pulses copropagating with infrared pulses after the input delays were set at 0 and 80 psec, respectively. The main effect of the nonlinear interaction was to shift the carrier frequency of green pulses. The induced wavelength shift versus the input delay between infrared and green pulses is plotted in Fig. 4. The maximum induced wavelength shift increased linearly with the infrared pulse peak power. Hence the carrier wavelength of green pulses could be tuned as much as 4 Å toward both the red and blue sides by varying the time delay between infrared and green pulses at the fiber input. [The solid curve in Fig. 4 is from the theory of Eqs. (8a) and (8b) below.] The nonlinear phase shifts and frequency chirps are given by[30]

$$\alpha_1(\tau, z) = -\sqrt{\pi}\,\frac{\omega_1}{c}\,n_2 E_2^{\,2} L_w \times\left[\operatorname{erf}(\tau-\tau_d)-\operatorname{erf}\left(\tau-\tau_d+\frac{z}{L_w}\right)\right], \tag{8a}$$

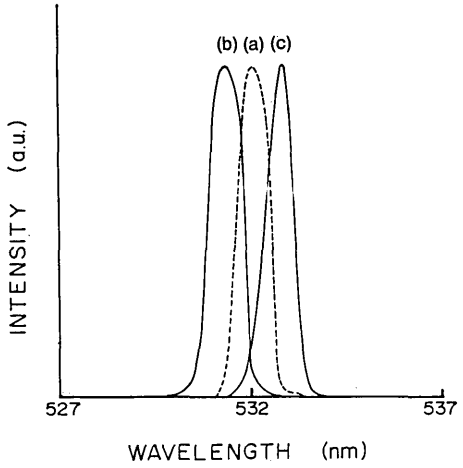

Fig. 3. XPM effects on spectra of green 532-nm pulses: (a) reference spectrum (no copropagating infrared pulse), (b) infrared and green pulses overlapped at the fiber input, (c) infrared pulse delayed by 80-psec at the fiber input.[30]

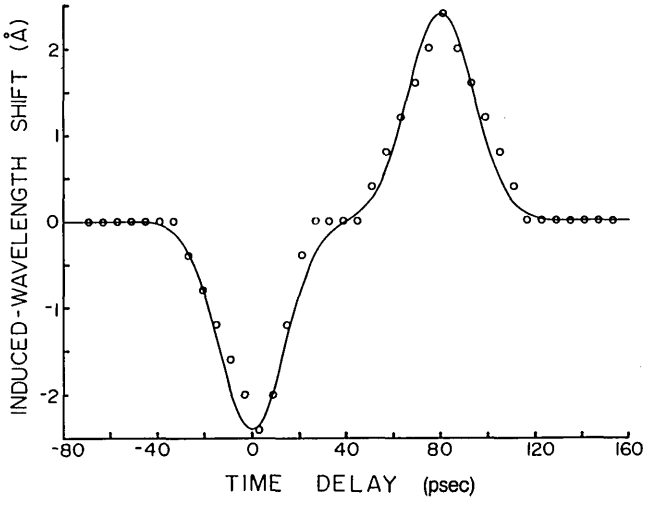

Fig. 4. Induced-wavelength shift of green 532-nm pulses as a function of the input time delay between 532-nm pulses and infrared 1064-nm pulses at the input of a 1-m-long optical fiber. Circles are experimental points. The solid curve is the theoretical prediction.[30]

$$\delta\omega_1(\tau, z) = 2\frac{\omega_1}{c} n_2 E_2{}^2 \frac{L_w}{T_0} \times \left\{\exp[-(\tau - \tau_d)^2] - \exp\left[-\left(\tau - \tau_d + \frac{z}{L_w}\right)^2\right]\right\} \quad (8b)$$

for weak probe pulses in which the self-phase modulation contribution can be neglected.

When the pulses coincide at the fiber entrance ($\tau_d = 0$) the point of maximum phase is generated ahead of the green-pulse peak because of the group-velocity mismatch. The green pulse sees only the trailing part of the XPM profile because it travels slower than the pump pulse. This leads to a blue induced-frequency shift. Similarly, when the initial delay is set at 80 psec, the infrared pulse just has sufficient time to catch up with the green pulse. The green pulse sees only the leading part of the XPM phase shift, which gives rise to a red induced-frequency shift. When the initial delay is approximately 40 psec, the infrared pulse has time to pass entirely through the green pulse. The pulse envelope sees a constant dephasing, and there is no shift of the green spectrum (Fig. 4).

Assuming that the central part of the pump pulses provides the dominant contribution to XPM, we set $\tau = 0$ in Eq. (8b) and obtain

$$\delta\omega_1(\tau, z) = 2\frac{\omega_1}{c} n_2 E_2{}^2 \frac{L_w}{T_0} \times \left\{\exp[-(\tau - \tau_d)^2] - \exp\left[-\left(\tau - \tau_d + \frac{z}{L_w}\right)^2\right]\right\}. \quad (9)$$

Equation (9) is plotted in Fig. 4. There is good agreement between this simple analytical model and experimental data. Note that only a simple parameter (i.e., the infrared peak power at the maximum induced-frequency shift) has been adjusted to fit the data. Experimental parameters were $\lambda = 532$ nm, $T_0 = 19.8$ psec (33 psec FWHM), $L_w = 26$ cm, and $z/L_w = 4$.

5. STIMULATED RAMAN SCATTERING WITH CROSS-PHASE MODULATION IN SINGLE-MODE OPTICAL FIBERS

Recently much theoretical and experimental research has investigated the effects of XPM during the generation and/or amplification of a Raman pulse by a pump pulse.[4–12] As a consequence of the nonlinear interaction, the phase of a weak Raman pulse is time modulated by the pump-pulse envelope, which modifies its spectral distribution and can favor the generation of Raman solitons. Figure 5 shows how the spectrum of a picosecond Raman pulse can be affected by XPM effects.[10] Figure 5(a) corresponds to the reference spectrum of a weak 25-psec pulse after propagation in a 10-m-long single-mode optical fiber. As shown in Fig. 5(b), a broad Raman line is generated when the energy of the input pulse is increased above the SRS threshold. The Raman line appears to be two to three times broader than the pump line, with an enhancement of Stokes frequencies for the highest pump powers [Figs. 5(c) and 5(d)]. These two features are characteristic of the XPM interaction. The extra broadening of the Raman line was predicted by our first theoretical analysis of XPM.[1] It corresponds to the factor of 2 of XPM in Eqs. (4). The asymmetric broadening results from the walkoff that occurs between the pump and Raman pulses during the generation process.

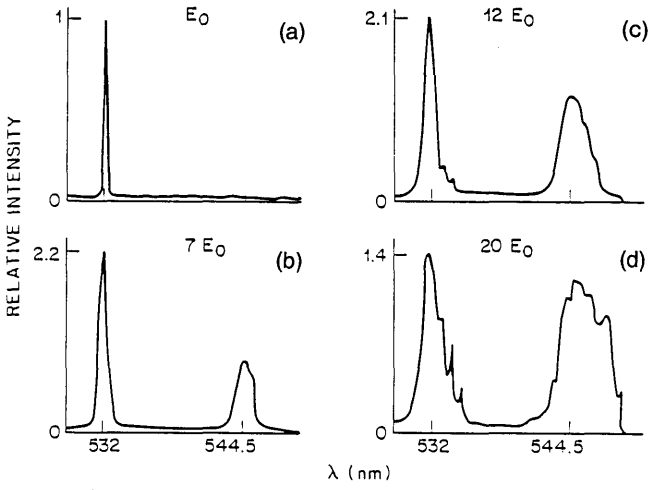

Fig. 5. Measured emission spectra of 25-psec laser pulses of different energies at 532-nm wavelength propagated through a 10-m-long single-mode glass fiber. The 544.5-nm peaks correspond to the peaks of the first Stokes Raman line.[10]

6. SECOND-HARMONIC CROSS-PHASE MODULATION

When intense ultrafast pulses propagate in a medium with $\chi^{(2)}$ and $\chi^{(3)}$ nonlinearities, XPM effects are more complex. In addition to spectral changes,[13] it has been shown that XPM generates the phase matching needed for SHG in non-phase-matched ZnSe crystals.[14–17] This affects the temporal profile of second-harmonic pulses.[14]

The temporal profile and propagation time of a 2-mJ 8-psec pump pulse at 1054 nm and its second-harmonic pulse generated through a 22-mm ZnSe polycrystalline sample are shown in Fig. 6.[14,15] A calibration pulse at 1054 nm is shown in Fig. 6(a). The second-harmonic signal whose spectrum spread from 500 to 570 nm indicated a sharp spike at 119 psec and a long plateau spanned over 60 psec [Fig. 6(b)]. Using 10-nm bandwidth narrow-band filters, we also measured pulses of selected wavelengths from the second-harmonic signal. Time delays corresponding to the propagation of two pulses with wavelengths centered at 530 and 550 nm are displayed in Figs. 6(c) and 6(d), respectively. As shown in Figs. 6(c) and 6(d), induced spectral-broadened pulses had one major component emitted at nearly the same time as the incident pulse [Fig. 6(a)].

The sharp spike and plateau of the second-harmonic pulse can be explained by using the XPM model of SHG.[17] Because of the lack of phase matching and destructive interference, the energy of the second-harmonic pulse cannot build up along the crystal length. As a result, most of the second-harmonic power is generated at the exit face of the crystal, which explains the observed spike. However, because intense pump pulses are involved, there is partial phase matching due to the XPM generated at the second-harmonic wavelength. Some second-harmonic energy can build up between the entrance and exit faces of the sample, which explains the plateau feature.

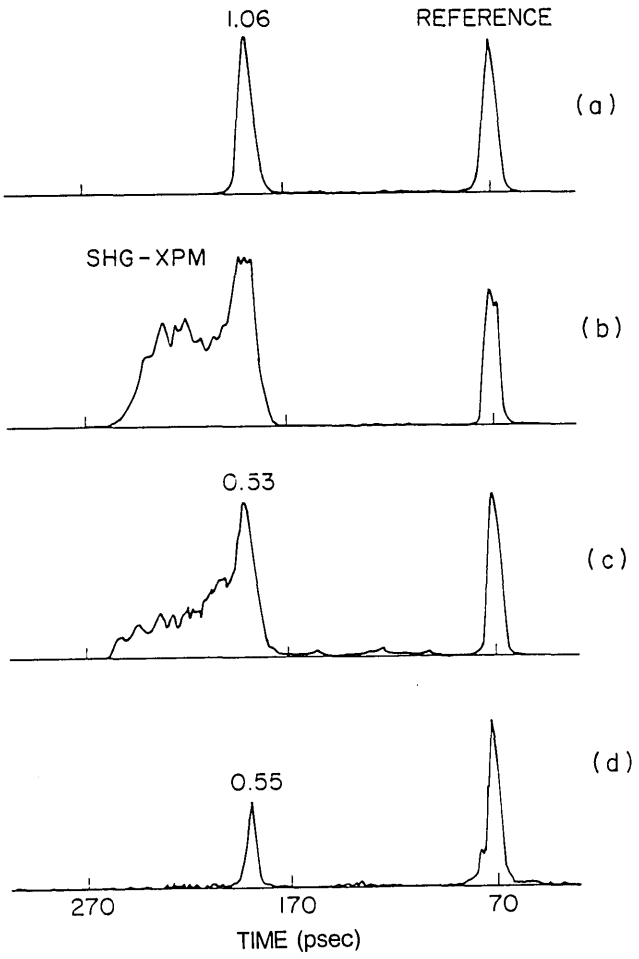

Fig. 6. Temporal profile and propagation delay time of (a) incident 1054-nm light; (b) SHG-XPM signal of all visible spectra; (c), (d) selected 530- and 550-nm lines from SHG-XPM of a 22-nm-long ZnSe crystal measured by a 2-psec resolution streak camera system. The reference time corresponds to a laser pulse traveling through air without the crystal. The right-hand side of the time scale is the leading time. The vertical scale is an arbitrary intensity scale.[14]

7. INDUCED FOCUSING OF PICOSECOND RAMAN PULSES IN OPTICAL FIBERS

Induced focusing is similar to the self-focusing of intense lasers beams, which was observed many years ago in liquids and solids. Induced focusing refers to the focusing of a probe beam occurring from the radial change of the refractive index induced by an intense copropagating pump beam. Recently experimental evidence for the focusing of picosecond pulses propagating in a 7.5-m-long 100-μm core-diameter optical fiber was reported.[32] Focusing occurred at Raman frequencies for which the spatial effect of the nonlinear refractive index was enhanced according to Eqs. (4). A decrease in the number of propagating modes occurring in SRS has also been observed in a previous experiment.[33]

Several magnified images of the intensity distributions that were observed at the output face of the fiber for different input pulse energies are shown in Fig. 7. The intensity distribution obtained for low pulse energies ($E < 1$ nJ) is shown in Fig. 7(a). It consists of a typical speckle pattern resulting from multimode interferences. Figure 7(b) shows the intensity distribution in the core for intense pulses ($E >$ 10 nJ). There is an intense, small (11-μm) ring of a Stokes-shifted frequency continuum of light at the center of the 100-μm fiber core. Approximately 50% of the input energy propagated in this small-ring pattern. In Fig. 7(c) a narrow-band filter selected the output light pattern at 550 nm. This clearly shows the ring distribution of the Stokes-shifted wavelengths.

The small-ring intensity profile is a signature of induced focusing at the Raman wavelengths. First, the small ring is speckleless, which is characteristic of single-mode propagation. This single-mode propagation means that the guiding properties of the fiber are dramatically changed by the incoming pulses, owing to SPM and XPM effects. Second, SRS, self-phase modulation, and XPM occur only in the ring structure, i.e., where the maximum of input energy has been concentrated. Third, a guided propagation in a ring structure is characteristic of a beam propagation in a graded-index fiber. Therefore our experimental results may be explained by an induced-gradient-index model for self-focusing, i.e., induced focusing. For high input energies the Gaussian beam induces a radial change of the refractive index in the optical-fiber core. The step-index fiber becomes a gradient-index fiber, which modifies its light-guiding properties. There is a further enhancement of the nonlinear refractive index at Raman frequencies because of XPM. Thus Stokes-shifted light propagates in a well-marked induced-gradient-index fiber.

In recent similar experiments the Raman pulse, propagating in the anomalous regime of a 500-m multimode fiber, was shown to form a femtosecond soliton (width, 70–100 fsec),

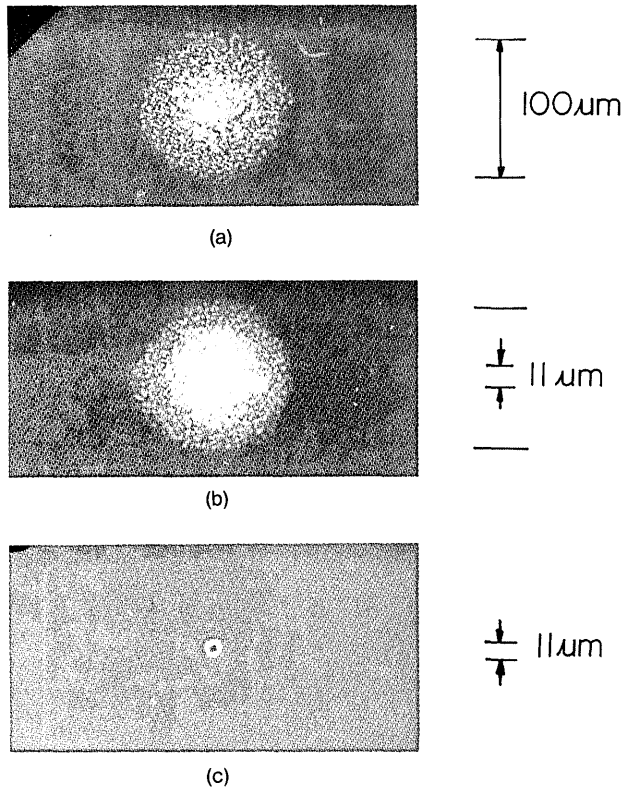

Fig. 7. Intensity distributions at the output of a large-core optical fiber: (a) input pulses of low energies ($E < 1$ nJ), (b) input pulses of high energies ($E > 10$ nJ), (c) same as (b) with an additional narrow-band filter centered at $\lambda = 550$ nm.[32]

which carried its energy in the fundamental fiber mode even though the 150-psec pump pulse excited a large number of the fiber modes.[34] This behavior could be a consequence of a nonlinear mode coupling, which prevents a diffusion of energy to higher-index modes. However, the physical mechanism for this coupling is not yet clear.[34]

8. CONCLUSION

We have demonstrated XPM and induced-focusing effects on copropagating picosecond pulses. The time and spatial dependences of the induced nonlinear refractive index $n_2|E(r, t)|^2$ can be used to control spectral, temporal, and spatial characteristics of ultrafast pulses. Potential applications are for spectral-broadening enhancement, pulse compression of weak pulses, frequency tuning, frequency multiplexing, and spatial modulation of ultrafast pulses with terahertz repetition rates.

ACKNOWLEDGMENTS

We gratefully acknowledge the partial support from the Hamamatsu K.K. and a faculty award from The City College of New York.

This paper was presented as an invited paper at the Optical Society of America Topical Meeting on Nonlinear Optical Properties of Materials, August 22–25, 1988, Troy, New York.

R. R. Alfano is also with the Department of Physics, The City College of New York.

REFERENCES

1. J. Gersten, R. R. Alfano, and M. Belic, "Combined stimulated Raman scattering and continuum self-phase modulation," Phys. Rev. A **21,** 1222–1224 (1980).
2. R. R. Alfano, Q. Li, T. Jimbo, J. Manassah, and P. P. Ho, "Induced spectral broadening of a weak picosecond pulse in glass produced by an intense picosecond pulse," Opt. Lett. **11,** 626–628 (1986).
3. J. T. Manassah, M. Mustafa, R. R. Alfano, and P. P. Ho, "Induced supercontinuum and steepening of an ultrafast laser pulse," Phys. Lett. **113A,** 242–247 (1985).
4. D. Schadt, B. Jaskorzynska, and U. Osterberg, "Numerical study on combined stimulated Raman scattering and self-phase modulation in optical fibers influenced by walk-off between pump and Stokes pulses," J. Opt. Soc. Am. B **3,** 1257–1260 (1986).
5. D. Schadt and B. Jaskorzynska, "Frequency chirp and spectra due to self-phase modulation and stimulated Raman scattering influenced by walkoff in optical fibers," J. Opt. Soc. Am. B **4,** 856–862 (1987).
6. M. N. Islam, L. F. Mollenauer, R. H. Stolen, J. R. Simson, and H. T. Shang, "Cross-phase modulation in optical fibers," Opt. Lett. **12,** 625–627 (1987).
7. M. N. Islam, L. F. Mollenauer, R. H. Stolen, J. R. Simson, and H. T. Shang, "Amplifier/compressor fiber Raman lasers," Opt. Lett. **12,** 814–816 (1987).
8. J. T. Manassah, "Induced phase modulation of the Raman pulse in optical fibers," Appl. Opt. **26,** 3747–3749 (1987).
9. J. T. Manassah, "Time-domain characteristics of a Raman pulse in the presence of a pump," Appl. Opt. **26,** 3750–3751 (1987).
10. R. R. Alfano, P. L. Baldeck, F. Raccah, and P. P. Ho, "Cross-phase modulation measured in optical fibers," Appl. Opt. **26,** 3491–3492 (1987).
11. P. L. Baldeck, P. P. Ho, and R. R. Alfano, "Effects of self induced, and cross phase modulations on the generation of picosecond and femtosecond white light supercontinua," Rev. Phys. Appl. **22,** 1677–1694 (1987).
12. A. Hook, D. Anderson, and M. Lisak, "Solitonlike Stokes pulses in stimulated Raman scattering," Opt. Lett. **13,** 1114–1116 (1988).
13. R. R. Alfano, Q. Z. Wang, T. Jimbo, and P. P. Ho, "Induced spectral broadening about a second harmonic generated by an intense primary ultrafast laser pulse in ZnSe crystals," Phys. Rev. A **35,** 459–462 (1987).
14. R. R. Alfano and P. P. Ho, "Self-, cross-, and induced-phase modulations of ultrashort laser pulse propagation," IEEE J. Quantum Electron. **QE-24,** 351–364 (1988).
15. P. P. Ho, Q. Z. Wang, D. Ji, and R. R. Alfano, "Propagation of harmonic cross-phase-modulation pulses in ZnSe," Appl. Phys. Lett. (to be published).
16. J. T. Manassah, "Amplitude and phase of a pulsed second-harmonic signal," J. Opt. Soc. Am. B **4,** 1235–1240 (1987).
17. J. T. Manassah and O. R. Cockings, "Induced phase modulation of a generated second-harmonic signal," Opt. Lett. **12,** 1005–1007 (1987).
18. P. L. Baldeck and R. R. Alfano, "Intensity effects on the stimulated four photon spectra generated by picosecond pulses in optical fibers," IEEE J. Lightwave Technol. **LT-5,** 1712–1715 (1987).
19. G. P. Agrawal, P. L. Baldeck, and R. R. Alfano, "Temporal and spectral effects of cross-phase modulation on copropagating ultrashort pulses in optical fibers," submitted to Phys. Rev. A.
20. G. P. Agrawal, "Modulation instability induced by cross-phase modulation," Phys. Rev. Lett. **59,** 880–883 (1987).
21. G. P. Agrawal, P. L. Baldeck, and R. R. Alfano, "Modulation instability induced by cross-phase modulation in optical fibers," Phys. Rev. A (to be published).
22. D. Schadt and B. Jaskorzynska, "Generation of short pulses from cw light by influence of cross-phase modulation in optical fibres," Electron. Lett. **23,** 1091–1092 (1987).
23. P. L. Baldeck, R. R. Alfano, and G. P. Agrawal, "Observation of modulation instability in the normal-dispersion regime of single-mode optical fibers," submitted to Opt. Lett.
24. A. S. Gouveia-Neto, M. E. Faldon, A. S. B. Sombra, P. G. J. Wigley, and J. R. Taylor, "Subpicosecond-pulse generation through cross-phase-modulation-induced modulation instability in optical fibers," Opt. Lett. **13,** 901–903 (1988).
25. A. S. Gouveia-Neto, M. E. Faldon, and J. R. Taylor, "Raman amplification of modulation instability and solitary-wave formation," Opt. Lett. **12,** 1029–1031 (1988).
26. S. Trillo, S. Wabnitz, E. M. Wright, and G. I. Stegeman, "Optical solitary waves induced by cross-phase modulation," Opt. Lett. **13,** 871–873 (1988).
27. B. Jaskorzynska and D. Schadt, "All-fiber distributed compression of weak pulses in the regime of negative group-velocity dispersion," IEEE J. Quantum Electron. **QE-24,** 2117–2120 (1988).
28. J. T. Manassah, "Pulse compression of an induced-phase modulated weak signal," Opt. Lett. **13,** 752–755 (1988).
29. G. P. Agrawal, P. L. Baldeck, and R. R. Alfano, "Optical wave breaking and pulse compression due to cross-phase modulation in optical fibers," Opt. Lett. **14,** 137–139 (1989).
30. P. L. Baldeck, R. R. Alfano, and G. P. Agrawal, "Induced-frequency shift of copropagating pulses," Appl. Phys. Lett. **52,** 1939 (1988).
31. D. Schadt and B. Jaskorzynska, "Suppression of the Raman self-frequency shift by cross-phase modulation," J. Opt. Soc. Am. B **5,** 2374–2378 (1988).
32. P. L. Baldeck, F. Raccah, and R. R. Alfano, "Observation of self-focusing in optical fibers with picosecond pulses," Opt. Lett. **12,** 588–589 (1987).
33. Z. V. Nesterova, I. V. Aleksandrov, A. A. Polnitskii, and D. K. Sattarov, "Propagation characteristics of high power ultrashort pulses in multimode optical fibers," JETP Lett. **34,** 371 (1981).
34. A. B. Grudinin, E. M. Dianov, D. V. Korbkin, A. M. Prokhorov, and D. V. Khaidarov, "Nonlinear mode coupling in multimode optical fibers; excitation of femtosecond-range stimulated-Raman-scattering solitons," JETP Lett. **47,** 356–359 (1988).